Supplementary Information

RNAi targeting sequences

The RNAi targeting sequences used in this study were as follows:

α3 integrin knockdown (α3-KD) cells, 5'-GGATGACTGTGAGCGGATGAA-3';

α3-KD2 cells, 5'-CAACGAGATGTGCAATAGCAA-3' (ULTRA-3316429);

RhoA sh1, 5'-GTACATGGAGTGTTCAGCAAA-3' (TRCN0000047710);

RhoA sh2, 5'-TGGAAAGACATGCTTGCTCAT-3' (TRCN0000047711);

RhoA sh3, 5'-GAAAGCAGGTAGAGTTGGCTT-3' (TRCN0000047712);

RhoC sh1, 5'-TGATGTCATCCTCATGTGCTT-3' (TRCN0000291516);

RhoC sh2, 5'-CTACTGTCTTTGAGAACTATA'-3' (TRCN0000047864);

LATS sh1, 5'-TATTCCTCAGTCTATGATGGT'-3';

LATS sh2, 5'-TTCCTGTTGGCAGACAACCAA-3';

LATS sh3, 5'-TTAACCGCAAACAGAGCTGGA-3';

LATS sh4, 5'-TACGAGTCAATCAGTAAGCCT-3';

LATS sh5, 5'-GAAGATAAAGACACTAGGAAT-3' (TRCN0000001776);

LATS sh6, 5'-CACGGCAAGATAGCATGGATT-3' (TRCN0000001777);

shYAP, 5'-CTGGTCAGAGATACTTCTTAA-3';

YAP sh1, 5'-ATACCTGATGATGTACCTCTG-3';

YAP sh2, 5'-ACAGGTGATACTATCAACCAA-3';

shTAZ, 5'-TGTCATGAATCCGAAGCCTAG-3';

TAZ sh1, 5'-TCCGGAGGACTTCCTCAGCAA-3' (ULTRA-3266816);

TAZ sh2, 5'-CACATAGAAAAAATCACCACA-3' (ULTRA-3266817);

TAZ sh3 5'-CCGGAGGACTTCCTCAGCAAT-3' (ULTRA-3266819);

Arg sh1, 5'-GTCCTTATCTCACCCACTC-3';

Arg sh2, 5'-CCTCAAACTCGCAACAAAT-3';

Abl sh1, 5-CCAGGTGTATGAGCTGCTAGA-3' (ULTRA-3267082);

Abl sh2, 5'-CAGGATCAACACTGCTTCTGA-3' (ULTRA-3267083);

Abl sh3, 5'-GCAGTCATGAAAGAGATCAAA-3' (ULTRA-3267084).

Supplementary Figure Legends

Figure S1. Stable silencing of α3 integrin in GS689.Li cells. RNAi silencing of α3 integrin in GS689.Li prostate cancer cells was evaluated by flow cytometry. The geometric mean fluorescence of α3 integrin staining was reduced by ~90% in the α3-KD cells.

Figure S2. Dissemination of α3-KD and NT control cells adjusted for primary tumor burden. (**A**) The apparent primary tumor burden in each mouse at the time of sacrifice was measured by drawing a region of interest over the site of tumor implantation and quantifying the total photon flux. Data are plotted as log photon flux. There was a trend towards higher tumor burden in the mice harboring the α3-KD prostate cancer cells, but the difference was not statistically significant. (**B**) Lung colonization data (μm^2 of area occupied by GFP-labeled cells) was normalized for the total primary tumor burden as measured by BLI. The α3-KD cell metastasis to lung was significantly greater than NT control cell metastasis, P=0.0493, unpaired t test. (**C**) Liver colonization (% area of liver surface occupied by GFP-labeled prostate cancer cells) was normalized to primary tumor burden. The α3-KD cells showed significantly more colonization, P=0.023, unpaired t test. (**D**) Kidney colonization (% area of kidney surface occupied by GFP-labeled prostate cancer cells) was normalized to primary tumor burden. The α3-KD cells showed a trend towards greater colonization, but the difference did not rise to statistical significance.

Figure S3. Silencing α3 integrin in multiple contexts promotes prostate carcinoma cell growth in 3D matrix. (**A**) An independent α3 integrin RNAi vector (α3-KD2) strongly blocked α3 integrin expression. *Top panel*: α3 integrin was immunoprecipitated from detergent extracts of NT control and α3-KD2 cells that had been cell surface labeled with biotin. *Middle panel*: total α3 integrin expression was measured by immunoblotting lysates of NT control and α3-KD cells. *Lower panel*: actin loading control. Numbers below each lane indicate intensity values obtained from a LiCOR blot imager. (**B**) The α3-KD2 cells showed significantly increased growth in 3D *P<0.0001, unpaired t test. (**C**) RNAi silencing of α3 integrin using the α3-KD construct in DU-145 prostate cancer cells was evaluated by flow cytometry. The geometric mean fluorescence of α3 integrin staining was reduced by ~89% in the α3-KD DU-145 cells. (**D**) The α3-KD DU-145 cells also displayed significantly increased growth in 3D, compared to the NT control cells *P<0.0001, unpaired t test.

Figure S4. The α3-KD cells display increased contractility, which contributes to growth under low growth factor and low anchorage conditions. (**A**) The α3-KD cells displayed a more profound contractile response to serum refeed after overnight serum starvation. (**B**) Quantification of spread cell area after serum refeed. *P=0.005, P=0.001, P=0.00004, P=0.0001, P=0.0001, and P=0.00003 at 5-10 minutes post-serum refeed, respectively, Holm-Sidak's multiple comparison test, α=0.05. Error bars, ± SEM, n=10. The myosin II inhibitor, blebbistatin, drove down the growth of α3-KD cells under serum starvation conditions in 2D cultures (**C**) or on 3D collagen (**D**); P values are from 2 way ANOVA with Tukey's multiple comparison test.

Figure S5. Increased TAZ expression in α3-KD DU-145 cells growing in suspension. DU145 NT control cells and α3-KD cells were cultured in suspension over non-adherent poly-HEMA for 4 days, lysed and immunoblotted for TAZ protein. TAZ protein levels were increased

in the α3-KD DU-145 cells, similar to the α3-KD GS689.Li prostate carcinoma cells. Actin loading controls are shown in the lower panel. Numbers below each lane indicate intensity units obtained with a LiCOR blot imager.

Figure S6. Increased RhoA activity and YAP and TAZ expression in α3-KD GS689.Li cells growing in suspension. α3-KD and NT control cells were grown for 3 days under detached conditions over poly-HEMA, as described in Materials and Methods. (**A**) Cell lysates were prepared from 3 biological replicates per cell type and used for Rhotekin-GST pulldown assays to measure active (GTP-loaded) RhoA and RhoC, or blotted for total RhoA, RhoC, YAP, TAZ, or tubulin. (**B-I**) Quantification of the blot shown in (A) using a LiCOR blot imager. Values in **B**, **C**, and **F-I** are normalized based on the tubulin loading control. Values in **D** and **E** are expressed as a ratio of active/total RhoA or RhoC. GTP-RhoA, YAP, and TAZ were all increased in α3-KD cells compared to NT control cells. P values from unpaired t test.

Figure S7. Silencing TAZ but not YAP with multiple independent constructs blocks the growth of α3-KD cells. (**A**) Evaluation of YAP and TAZ protein expression levels in α3-KD cells transduced with a non-targeting (NT) control construct or with one of three different TAZ shRNA constructs. TAZ expression was reduced by 88-90% in TAZsh1 and TAZsh2 cells, and by 62% in TAZsh3 cells. Lower panel shows actin loading controls. Numbers below each lane indicate intensity units from a LiCOR blot imager. (**B**) The α3-KD cells depleted for TAZ all showed significantly reduced 3D growth compared to the NT control cells, ***P<0.0001, ANOVA with Tukey post-test. In addition, TAZsh3 cells, which retained somewhat more TAZ expression, showed a modest but significant increase in 3D growth compared to TAZsh1 and TAZsh2, P=0.0015 and 0.0008 respectively, ANOVA with Tukey post-test. (**C**) Evaluation of YAP protein expression in α3-KD cells transduced with a non-targeting (NT) control construct or with one of

two different TAZ shRNA constructs. YAP expression was reduced by 77% and 83% in YAPsh1 and YAPsh2 cells respectively. (**D**) Neither YAP shRNA construct reduced 3D growth; instead, each construct appeared to moderately increase growth.

Figure S8. Involvement of LATS1 in suppression of 3D growth mediated by α3 integrin. (**A&B**) The LATS1 sh4 construct reduced LATS1 expression by ~90%, and potently promoted the growth of the cells in 3D collagen, P<0.0001, ANOVA with Tukey's post test. (**C&D**) Force-expressing LATS1 in α3-KD cells increased LATS1 protein levels by ~87% and suppressed 3D growth; P=0.0023, unpaired t test. (**E&F**) The LATS sh5 construct reduced LATS1 expression by ~67% and moderately increased 3D growth compared to non-targeting vector control (VEC) or the inactive LATS sh6 construct, P values from ANOVA with Tukey's post test.

Figure S9. p190RhoGAP activation state is reduced in α3-KD cells growing in suspension. NT control and α3-KD cells were grown in suspension over non-adherent poly-HEMA in serum-free medium with 5 μM LPA for 4 days. (**A**) Cell lysates were prepared and p190RhoGAP was immunoprecipitated, followed by blotting for (i) phospho-tyrosine to detect phosphorylated, activated p190 (upper panel), (ii) p120RasGAP to detect the p190/p120 complex (middle panel), or (iii) total p190RhoGAP as a loading control (lower panel). The amount of phosphorylated, p120-associated p190 was reduced in the α3-KD cells. (**B**) Blotting for phospho-Crk/CrkL (upper panel) or total Crk (lower panel). The amount of phospho-Crk/CrkL was reduced in the α3-KD cells, providing further evidence of reduced activity of Abl family kinase activity. Numbers below each lane in A and B are from a LiCOR blot imager.

Figure S10. FAK activation is increased in α3-KD cells growing under detached conditions, but a FAK inhibitor does not block 3D growth. (**A**) NT control and α3-KD cells

were grown for 4 days under detached conditions, as described in Materials and Methods and cell lysates were blotted for phospho-FAK (Y397), total FAK, or actin. (**B**) Dose-response effect of FAK inhibitor PF-573228 on growth in 3D collagen.

Figure S11. Quartile scoring system for the prostate cancer tissue microarray. (**A**) Representative images of the quartile scoring system developed for α3 integrin, and nuclear TAZ and YAP (see Materials and Methods for details). (Note: proliferative basal cells in benign glands are TAZ and YAP positive). (**B**) The anti-α3 integrin, anti-TAZ, and anti-YAP antibodies used for IHC analysis each recognized a major band of the appropriate size in immunoblots of GS689.Li control cell lysates that was absent in the respective α3, TAZ, or YAP-silenced GS689.Li cell lysates.

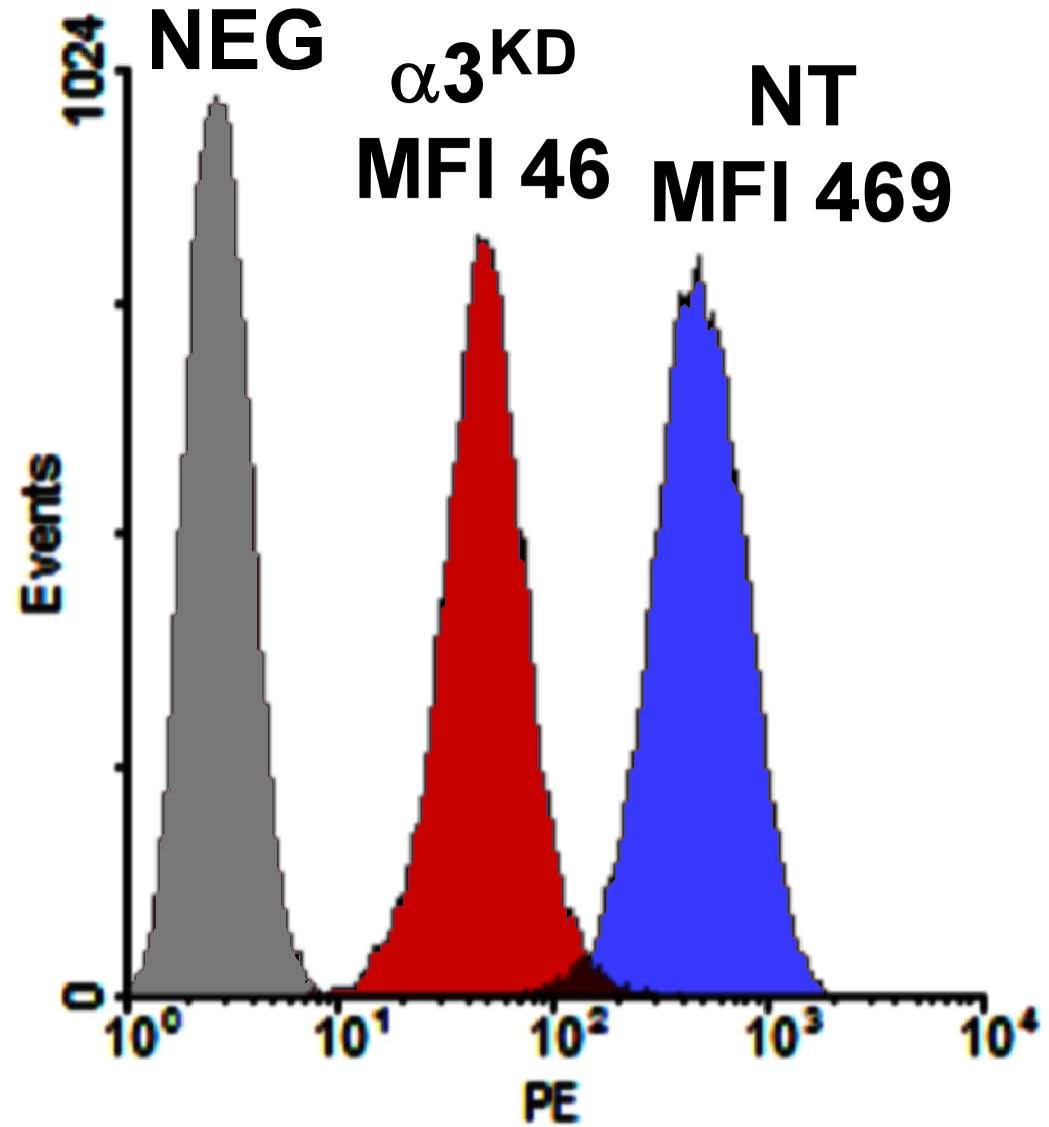

Figure S1

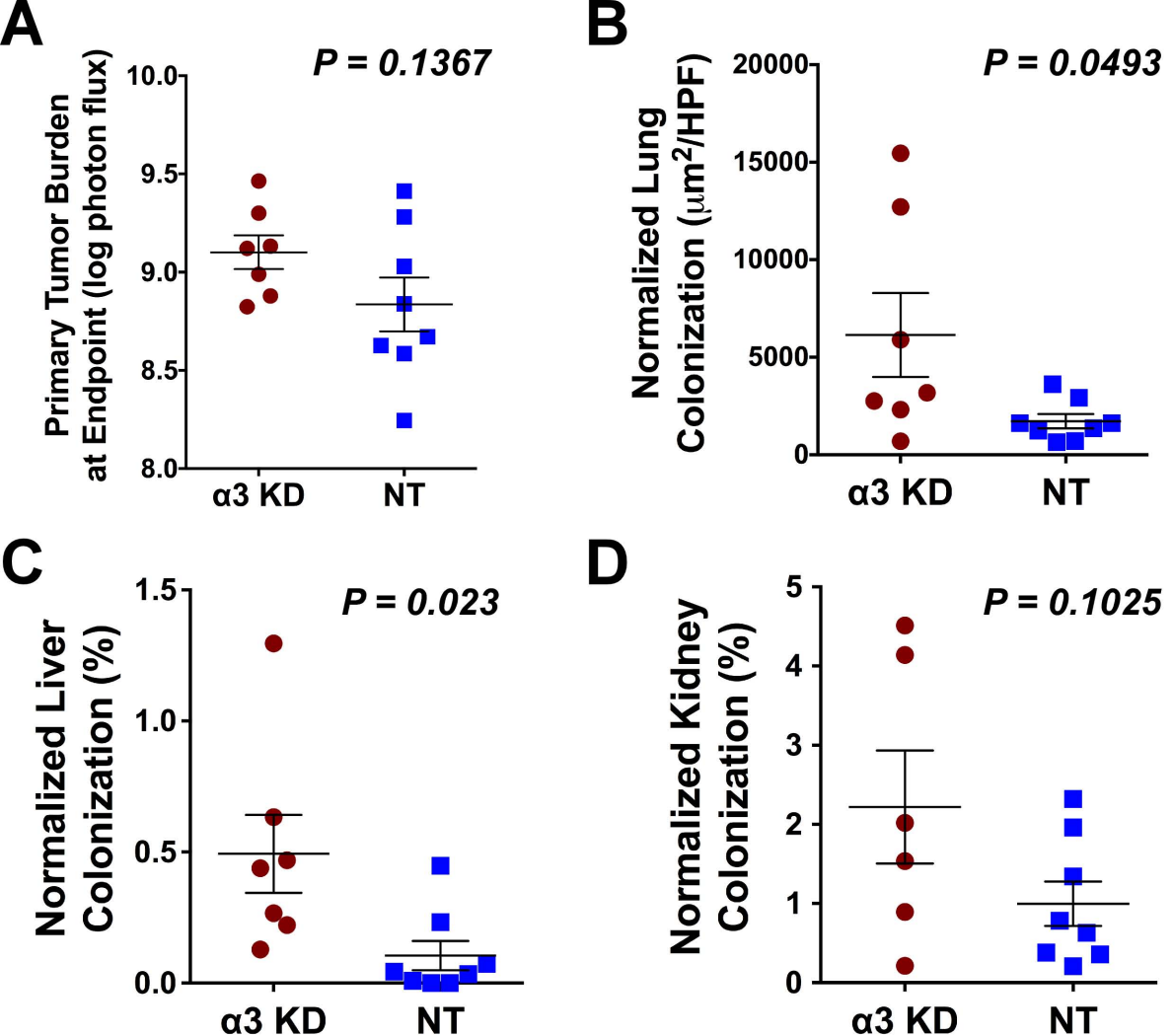
A
Primary Tumor Burden at Endpoint (log photon flux)
P = 0.1367
10.0
9.5
9.0
8.5
8.0
α3 KD
NT
B
Normalized Lung Colonization (μm²/HPF)
P = 0.0493
20000
15000
10000
5000
0
α3 KD
NT
C
Normalized Liver Colonization (%)
P = 0.023
1.5
1.0
0.5
0.0
α3 KD
NT
D
Normalized Kidney Colonization (%)
P = 0.1025
5
4
3
2
1
0
α3 KD
NT

Figure S2

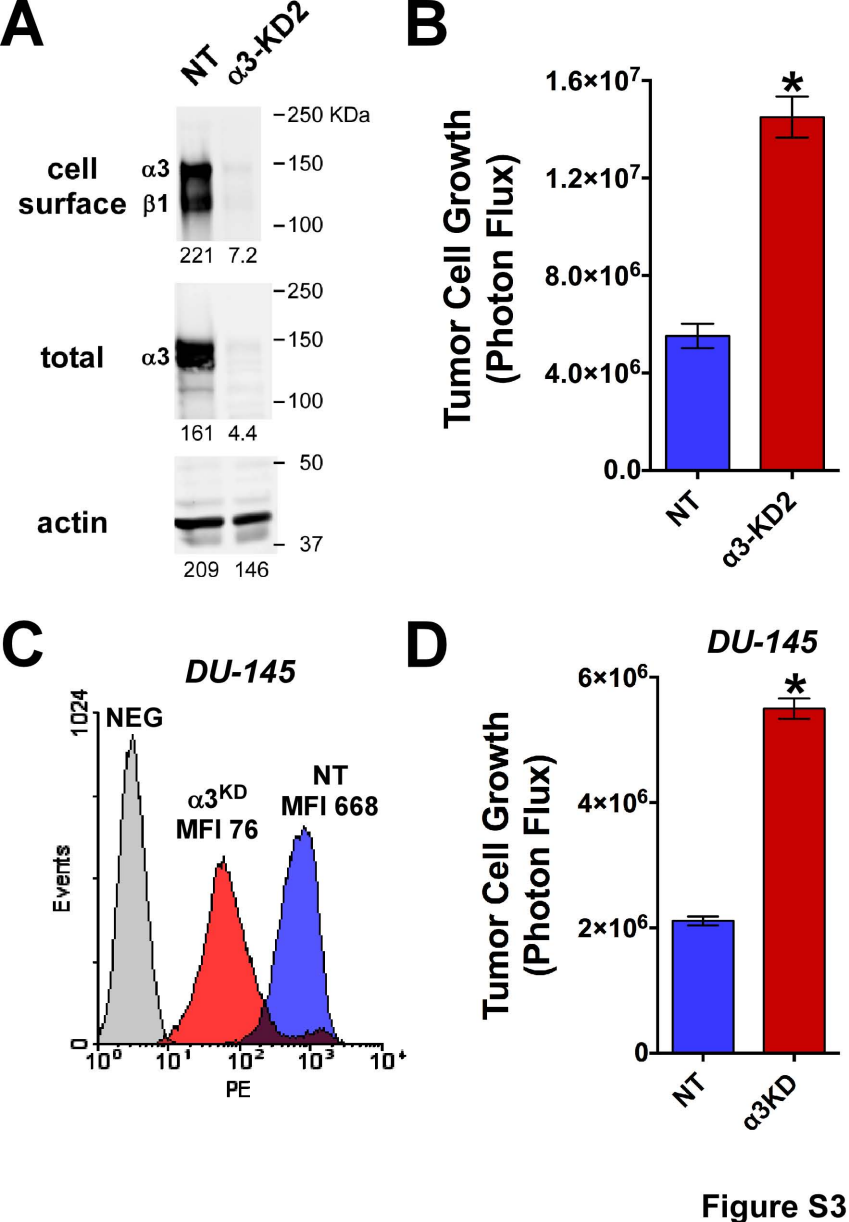
A
NT
α3-KD2
250 KDa
150
100
cell surface
α3
β1
221 7.2
250
150
100
total
α3
161 4.4
50
actin
37
209 146
B
Tumor Cell Growth (Photon Flux)
1.6×10^7
1.2×10^7
8.0×10^6
4.0×10^6
0.0
*
NT
α3-KD2
C
DU-145
NEG
α3^KD MFI 76
NT MFI 668
1024
Events
0
10^0
10^1
10^2
10^3
10^4
PE
D
DU-145
Tumor Cell Growth (Photon Flux)
6×10^6
4×10^6
2×10^6
0
*
NT
α3KD

Figure S3

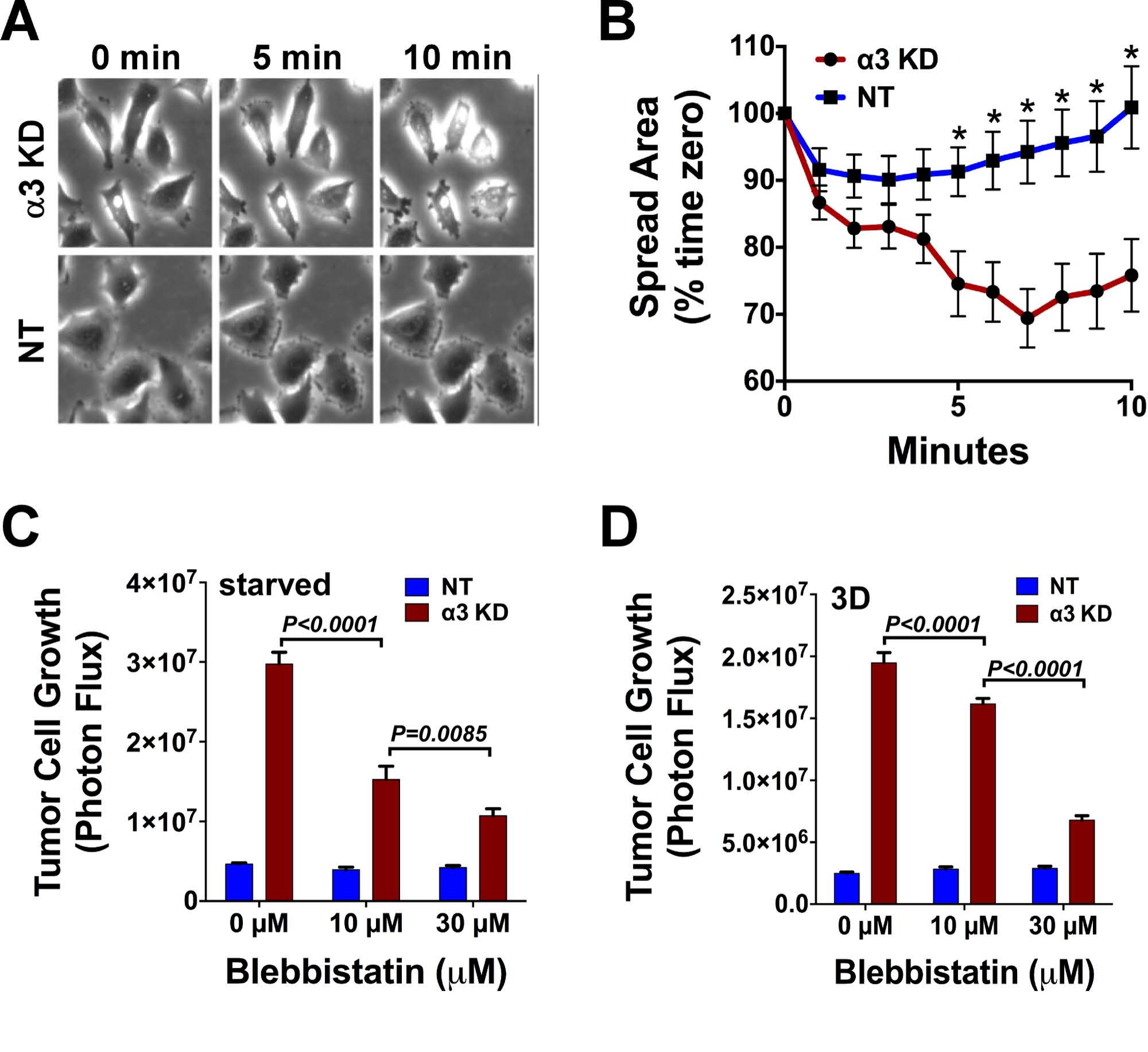
A
0 min
5 min
10 min
α3 KD
NT
B
α3 KD
NT
Spread Area (% time zero)
110
100
90
80
70
60
0
5
10
Minutes
*
C
starved
NT
α3 KD
P<0.0001
P=0.0085
Tumor Cell Growth (Photon Flux)
4×10^7
3×10^7
2×10^7
1×10^7
0
0 μM
10 μM
30 μM
Blebbistatin (μM)
D
3D
NT
α3 KD
P<0.0001
P<0.0001
Tumor Cell Growth (Photon Flux)
2.5×10^7
2.0×10^7
1.5×10^7
1.0×10^7
5.0×10^6
0.0
0 μM
10 μM
30 μM
Blebbistatin (μM)

Figure S4

Figure S5

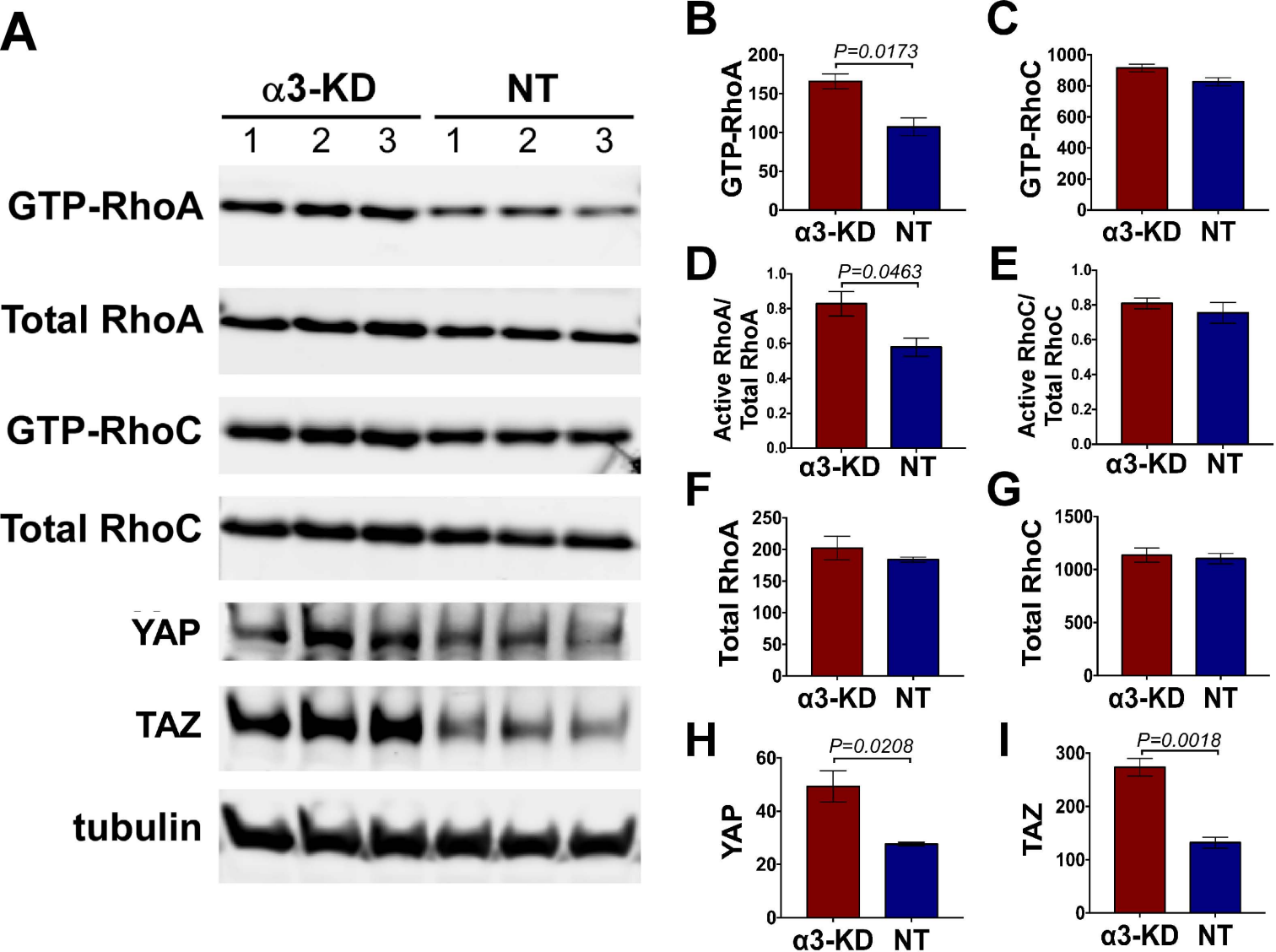
A
α3-KD
NT
1 2 3 1 2 3
GTP-RhoA
Total RhoA
GTP-RhoC
Total RhoC
YAP
TAZ
tubulin
B
GTP-RhoA
P=0.0173
α3-KD NT
C
GTP-RhoC
α3-KD NT
D
Active RhoA/ Total RhoA
P=0.0463
α3-KD NT
E
Active RhoC/ Total RhoC
α3-KD NT
F
Total RhoA
α3-KD NT
G
Total RhoC
α3-KD NT
H
YAP
P=0.0208
α3-KD NT
I
TAZ
P=0.0018
α3-KD NT

Figure S6

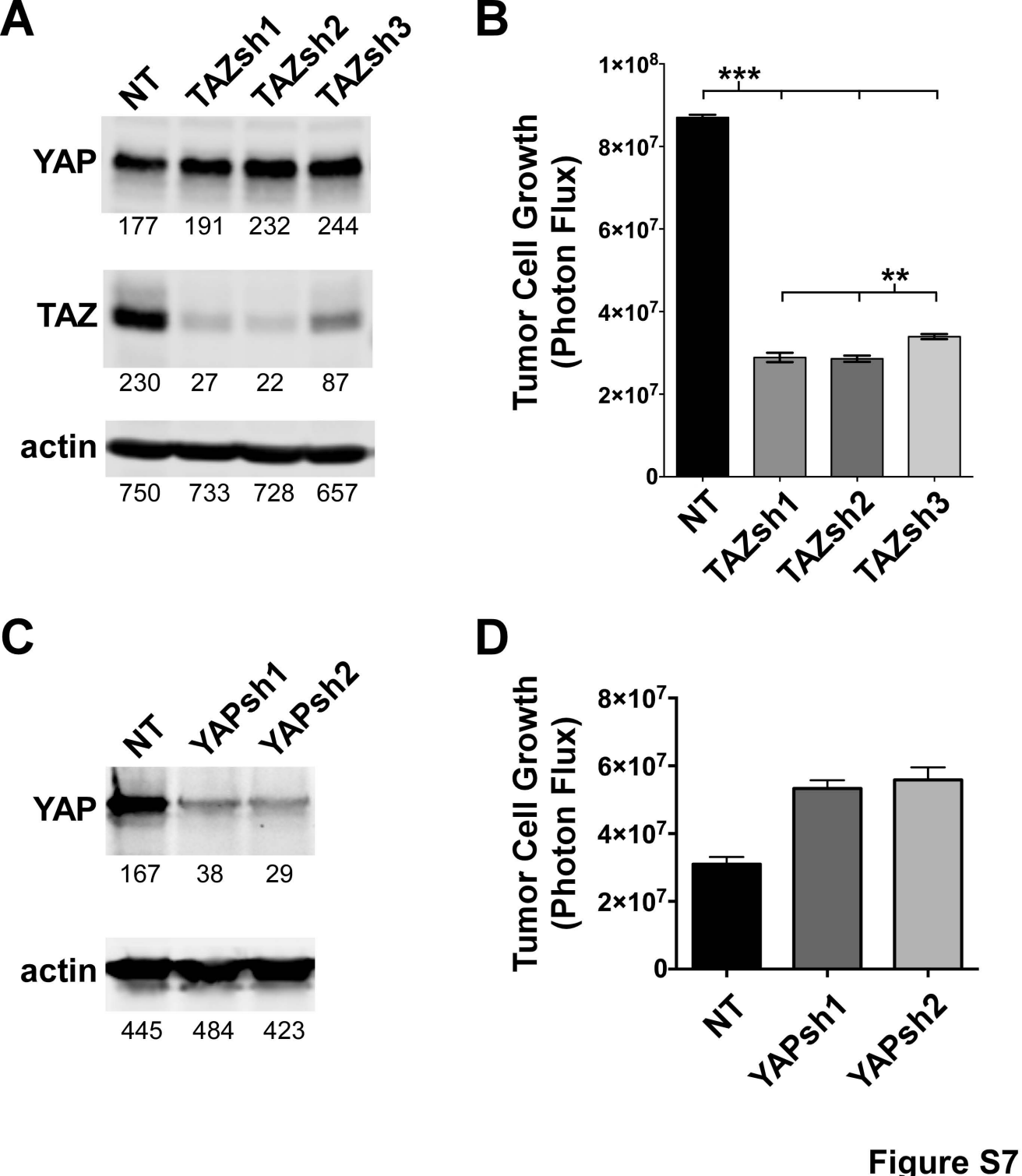
A
NT
TAZsh1
TAZsh2
TAZsh3
YAP
177 191 232 244
TAZ
230 27 22 87
actin
750 733 728 657
B
Tumor Cell Growth (Photon Flux)
1×10^8
8×10^7
6×10^7
4×10^7
2×10^7
0
***
**
NT
TAZsh1
TAZsh2
TAZsh3
C
NT
YAPsh1
YAPsh2
YAP
167 38 29
actin
445 484 423
D
Tumor Cell Growth (Photon Flux)
8×10^7
6×10^7
4×10^7
2×10^7
0
NT
YAPsh1
YAPsh2

Figure S7

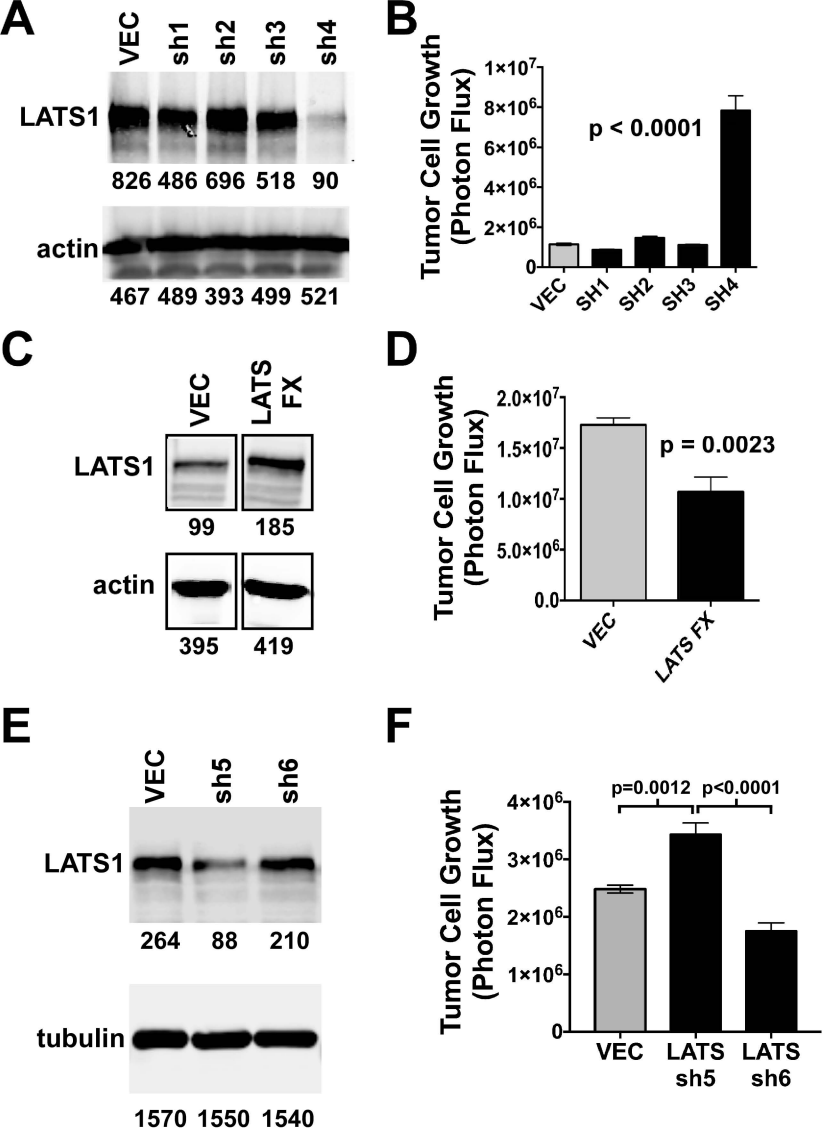
A
VEC
sh1
sh2
sh3
sh4
LATS1
826 486 696 518 90
actin
467 489 393 499 521
B
Tumor Cell Growth (Photon Flux)
1×10^7
8×10^6
6×10^6
4×10^6
2×10^6
0
p < 0.0001
VEC
SH1
SH2
SH3
SH4
C
VEC
LATS FX
LATS1
99
185
actin
395
419
D
Tumor Cell Growth (Photon Flux)
2.0×10^7
1.5×10^7
1.0×10^7
5.0×10^6
0.0
p = 0.0023
VEC
LATS FX
E
VEC
sh5
sh6
LATS1
264 88 210
tubulin
1570 1550 1540
F
Tumor Cell Growth (Photon Flux)
p=0.0012
p<0.0001
4×10^6
3×10^6
2×10^6
1×10^6
0
VEC
LATS sh5
LATS sh6

Figure S8

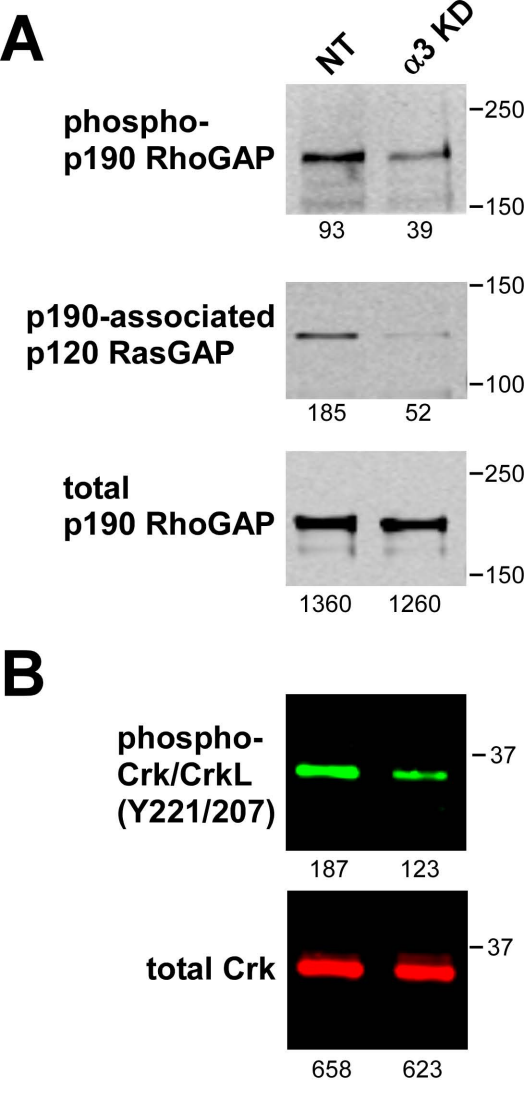
A
NT
α3 KD
phospho-
p190 RhoGAP
250
150
93
39
p190-associated
p120 RasGAP
150
100
185
52
total
p190 RhoGAP
250
150
1360
1260
B
phospho-
Crk/CrkL
(Y221/207)
37
187
123
total Crk
37
658
623

Figure S9

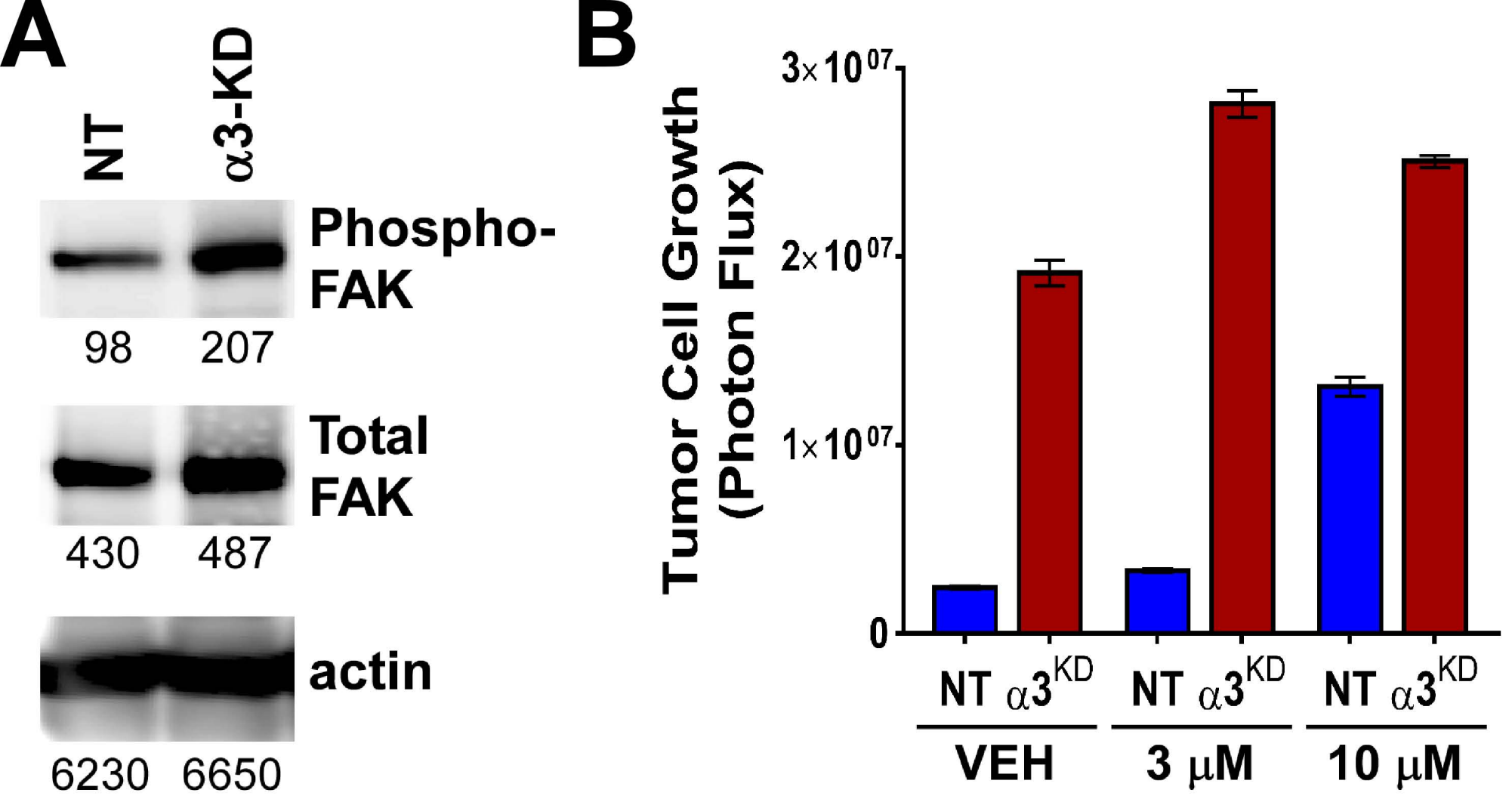
A
NT
α3-KD
Phospho-FAK
98
207
Total FAK
430
487
actin
6230
6650
B
Tumor Cell Growth (Photon Flux)
3×10^07
2×10^07
1×10^07
0
NT α3^KD
NT α3^KD
NT α3^KD
VEH
3 μM
10 μM

Figure S10

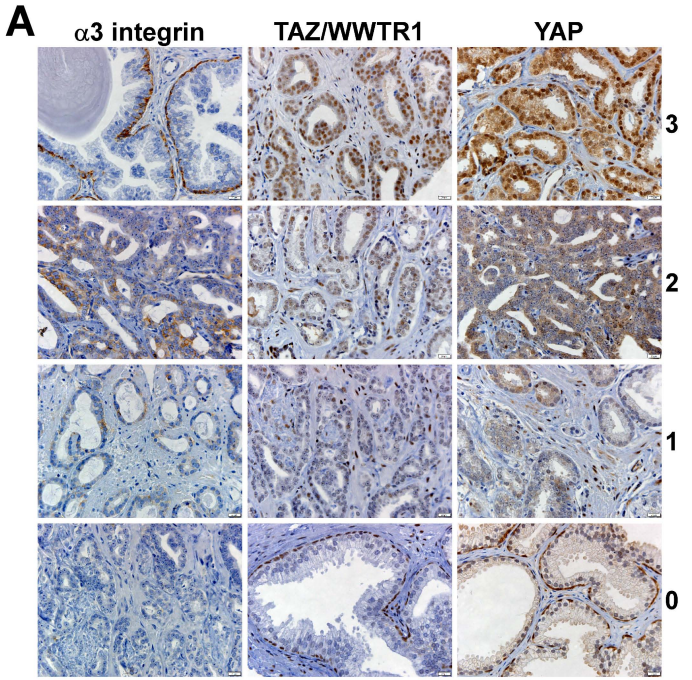
A
α3 integrin
TAZ/WWTR1
YAP
3
2
1
0

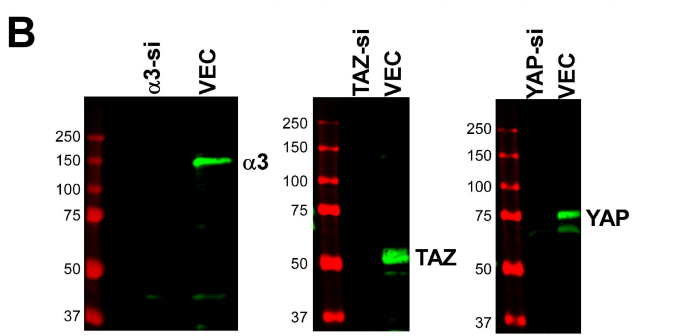
B
α3-si
VEC
TAZ-si
VEC
YAP-si
VEC
250
150
100
75
50
37
α3
TAZ
YAP

Figure S11